IEEE Access
Multidisciplinary | Rapid Review | Open Access Journal

Received February 17, 2018, accepted April 5, 2018, date of publication April 23, 2018, date of current version May 16, 2018.

Digital Object Identifier 10.1109/ACCESS.2018.2829148

Methodology for Flicker Estimation and Its Correlation to Environmental Factors in Photovoltaic Generation

DAVID A. ELVIRA-ORTIZ[1], (Student Member, IEEE), DANIEL MORINIGO-SOTELO[2], (Member, IEEE), OSCAR DUQUE-PEREZ[2], ARTURO Y. JAEN-CUELLAR[1], ROQUE A. OSORNIO-RIOS[1], (Member, IEEE), AND RENE DE J. ROMERO-TRONCOSO[1], (Senior Member, IEEE)

[1]HSPdigital–CA Mecatronica, Facultad de Ingenieria, Autonomus University of Queretaro, Campus San Juan del Rio, 76807 San Juan del Rio, Mexico
[2]HSPdigital–Department of Electrical Engineering, University of Valladolid, 47011 Valladolid, Spain

Corresponding author: Daniel Morinigo-Sotelo (dmorinigo@hspdigital.org)

This work was supported in part by the CONACYT Scholarship under Grant 415315, in part by FOMIX under Grant QUERETARO-2014-C03-250269, and in part by CEI-Triangular, Universidades de Burgos, León y Valladolid.

ABSTRACT Flicker is a very common power quality disturbance due to the inclusion of photovoltaic (PV) generation on the electric grid. This paper presents a methodology for flicker estimation in a PV generation that fuses multiple signal classification and discrete wavelet transform to provide high-resolution frequency estimation with an accurate amplitude measurement. This tool considers that flicker is not stationary over time and that more than one frequency component can exist on a voltage signal. In Addition, this paper finds that sun irradiance, temperature, and the action of the solar inverter are the sources of flicker in PV generation. The methodology is applied to real signals from three days with different weather conditions. In Addition, two different solar inverters are evaluated to see their influence on the parameters of flicker. Results show that flicker can contain more than one frequency component that can change over time. Finally, this paper shows that around 70% to 80% of flicker is linked to irradiance and cell temperature whereas the 20% to 30% can be attributed to the operation of solar inverters.

INDEX TERMS Discrete wavelet transforms, flickr, multiple signal classification, photovoltaic systems, power quality.

I. INTRODUCTION

Renewable energies have become very important in modern society as an alternative to conventional generation sources that have been robust and reliable power supplies for many years; yet, this type of generation is carried out through fossil fuels, which are non-renewable and therefore, finite. Moreover, gases from the combustion of these fuels have led to a series of environmental issues such as climate changes and depletion of the protective ozone layer, representing a risk to human health. In this sense, renewable energies come from inexhaustible sources at a human scale and can be used with zero or almost zero emission of gases [1]. Among all the renewable energies, solar photovoltaic (PV) is one of the most widespread power technologies due to its modularity, free-maintenance and quiet performance [2]. However, the inclusion of solar PV energy involves some important challenges, for instance, solar PV cells deliver DC power, making necessary the use of a power inverter to properly supply the produced energy into the grid [3]. Additionally, the PV production fluctuates because it depends on atmospheric conditions like the solar irradiance that reaches the PV cell, the presence of clouds, and the temperature of the cell, among others [4], [5]. The use of power electronic devices and the dependence of weather conditions can lead to periodical local voltage variations that cause an undesired effect known as flicker [6], [7].

Flicker is a low-frequency voltage fluctuation that gives rise to noticeable illumination changes in lighting equipment [8] and is mainly caused by the use of non-linear and electronically-commutated loads that introduce high harmonic and interharmonic content to the voltage signal [9]–[11]. The admissible levels, as well as

a methodology to obtain a flickermeter (i.e., a device for flicker measurement), are described by the standard IEC 61000-4-15 [12]. However, this flickermeter presents certain limitations that can affect the proper measurement of the flicker [13], [14]. Since flicker is a phenomenon that modulates in amplitude the voltage signal, it is required to know the waveform of the modulating signal. Some works have developed analytic representations to measure and describe flicker. These works go from a simple frequency [15]–[17] or time-frequency [18], [19] analytic representations of the IEC flickermeter, to a complex and complete mathematical expression that describes, not only flicker, but a large set of power quality disturbances [20]. The mathematical approach in [20] is probably the most complete representation of power quality disturbances so far, and it certainly describes flicker as a waveform that modulates the amplitude of the voltage signal. However, no information is provided on how to extract or assess the parameters that compose the modulating signal. Other works use methodologies like the Hilbert transform to obtain the envelope of the voltage signal and then get the amplitude and frequency of the flicker using the fast Fourier transform (FFT) and the empirical mode decomposition [21]–[23]. Moreover, it is well known that flicker can cause irritation to the human brain, and there are also critical loads that demand a high-quality voltage supply, and that can be seriously affected by flicker [24]. Thereby, several techniques and methodologies have been developed to diminish flicker levels. The most common solutions are the use of smart loads [25], static synchronous compensators [26]–[28] or distribution static compensators [29], [30] for reactive power compensation. Although all the works above suitably assess the flicker sensation, they present some disadvantages. For instance, most of the reported works consider that flicker is composed by only one frequency, and only the amplitude for the flicker is reported. In [23] it is proposed a methodology that considers the existence of many frequency components in the envelope of the voltage signal using the FFT to find the frequency and amplitude of every flicker component. The use of the FFT in this methodology supposes that the signal is stationary, which is not true in most cases. Moreover, by estimating the frequency content through the FFT, the method implies that all components are exact multiple integers of the frequency resolution; otherwise, the estimated amplitude values will be erroneous due to spectral leakage. Then, it is necessary the use of a different technique that allows obtaining a better estimation of the frequencies and amplitudes of the flicker signal.

Regarding the specific causes of flicker in the PV generation, it has been noticed that changes in the solar irradiance due to clouds can lead to an increase of flicker levels [31]. Some works mention that solar irradiance is not fully predictable, resulting in intermittent power generation on cloudy days, where the voltage levels are fluctuating according to the changes of solar irradiation. This may affect the network voltage profile and cause voltage flicker [32]–[36]. These works present plots of the irradiance profile throughout the day and show that flicker levels are different from a sunny day to a cloudy day. Although these works show that there is a relationship between the irradiance and the flicker, the analysis is only qualitative. It is necessary to use statistical models to quantify how much the irradiance affects the flicker levels. This would allow determining if the irradiance is the only source of flicker on the PV generation or if there are some other factors that can influence this undesired effect. It is important to mention that so far, the reviewed works have studied the affection of the irradiance on flicker level, but they do not consider the temperature of the photovoltaic cell. Another well-known source of flicker is the interharmonic content of the voltage signal [37], [38]. According to [38], one of the mechanisms for the generation of interharmonics is the asynchronous commutation of semiconductor devices in static converters. Typical examples are cycloconverters and pulse-width modulation (PWM) converters. This is worth noticing because, in PV generation, the use of solar inverters is inevitable. Solar inverters are power electronic devices and they use PWM modules for their operation. In this sense, it is possible that the solar inverter itself is a source of flicker [6], [35].

This paper presents a methodology that estimates the flicker considering the existence of several frequency components, harmonics and interharmonics, on the flicker signal. The proposed method extracts the modulating signal that contains the low-frequency flicker components by a nonlinear demodulation that uses Hilbert transform to estimate the envelope of the voltage signal. Then, using the multiple signal classification (MUSIC) algorithm for spectral-analysis, all the frequency components of the envelope can be identified with a very high resolution. Since MUSIC does not deliver a good estimation about the signal energy, the discrete wavelet transform (DWT) is used to decompose the envelope of the voltage signal in modes to estimate the amplitude of every flicker component. This methodology is applied to two different solar inverters to show the contribution of the solar inverter on the flicker level. To assess only the flicker due to PV generation, the experiment is performed on a PV network that is connected to the distribution grid, but no significant loads exist in this node of the grid. Finally, using a linear regression model, the relationship between solar irradiance, cell temperature and flicker level is established. Results prove that the temperature of the cell and the irradiance explain a part of the flicker level and also that the solar inverter has a critical influence.

II. THEORETICAL BACKGROUND

A. FLICKER DEFINITION

The IEEE-1159 standard defines flicker as the impression of unsteadiness of visual sensation induced by a light stimulus whose luminance or spectral distribution fluctuates with time [39]. This sensation is due to voltage fluctuations on electric power systems, generating a waveform that modulates the amplitude of the voltage signal. This modulating waveform is characterized by presenting a frequency,

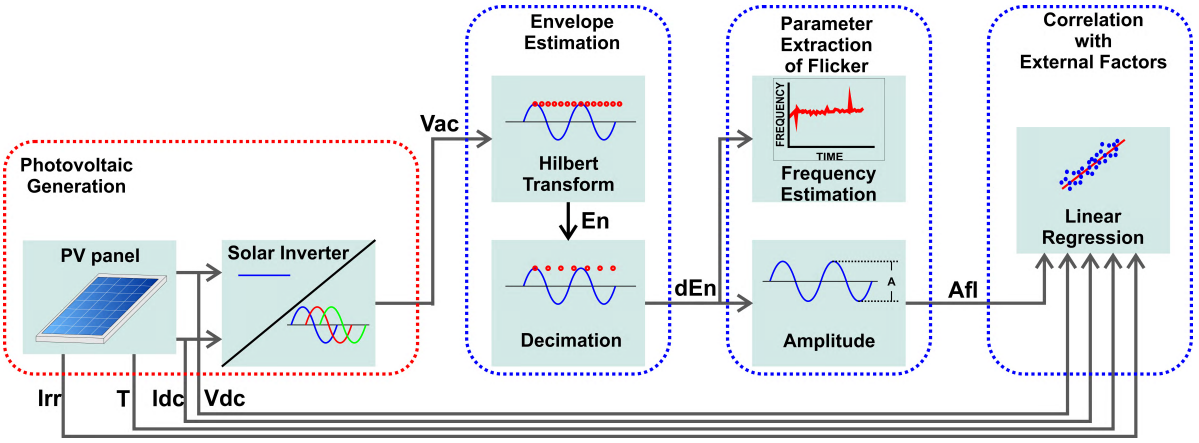

FIGURE 1. Methodology for the parameter extraction of flicker.

or a set of frequencies, that is lower than the fundamental supply frequency. However, certain combinations of frequency and amplitude of the modulating waveform can result in irritation for the people. In [20] it is presented a mathematical expression for flicker modeling. This representation considers well-defined parameters such as severity, DV/V, flicker frequency and duration of the event. The analytic approach is shown in (1)

$$X_{fl}(t) = A \cdot [1 + \delta_a(t)] \cdot [cos(2\pi f_0 t + \theta)] \quad (1)$$

where $X_{fl}(t)$ is the signal with flicker, A and f_0 are the amplitude and the frequency of the fundamental signal, and δ_a is a square modulation given by (2)

$$\delta_a(t) = A_{fl} \cdot sgn[\cos(2\pi f_{fl} t + \theta_{fl})] \quad (2)$$

being A_{fl} the amplitude of a square signal for modulation, directly related to the term DV/V. The function $sgn()$ is the sign function. The modulation has a frequency f_{fl} and phase θ_{fl}. It is important to mention that the model from (2) considers that the modulating signal contents only one frequency. However, (2) can be easily modified for considering the existence of several frequency components on the modulating signal as presented in (3)

$$\delta_a(t) = \Sigma_{i=1}^{n} A_{fl}(i) \cdot sgn\{\cos[2\pi f_{fl}(i) t + \theta_{fl}(i)]\} \quad (3)$$

where $A_{fl}(i)$ is the amplitude of the i-th component of the modulating signal with frequency $f_{fl}(i)$ and phase $\theta_{fl}(i)$. Therefore, it is possible to describe and represent every flicker signal by knowing the amplitude and the frequency of every component of the modulating signal. In this sense, it is necessary a methodology for estimating the modulating signal and accurately extracting its components.

B. STANDARD IEC 61000-4-15

The standard IEC 61000-4-15 [12] establishes the basis for the design of a fully functional measuring device, which purpose is correctly indicating the flicker perception level in a fluctuating voltage signal. This measuring device is called the flickermeter. Additionally, the standard provides a methodology to evaluate the flicker severity on the basis of the output provided by the flickermeter. Basically, the flickermeter is composed by 5 modules: a normalization module, a squaring multiplier, weighting filters, squaring and smoothing, and online statistical analysis. In the first module, the voltage signal is normalized using its own rms value. The second module squares the normalized voltage signal and converts the AC to DC signal, making it suitable for filtering. The weighting filters are the third block, and it is used to simulate the human eye response with a lamp. In this block, a first order high-pass filter with cutoff frequency of 0.05 Hz is used for filtering the DC component. Since flicker is a phenomenon with frequencies lower than the fundamental, the next step consists on filtering the frequencies higher than 35 Hz. A 6-th order low-pass filter is used for this purpose. Then a weighting filter is designed for removing the frequency components that cannot be appreciated by the human eye. In the next block, the signal is squared to simulate the eye-brain perception. Then, a filter with time constant of 300 ms is used for smoothing the signal. The output of this block is the instantaneous flicker (P_{inst}), and simulates the brain storage process for optic perception. Finally, in block 5 it is performed a statistical analysis for assessing the voltage flicker severity based on P_{inst}. This block delivers two outputs: the short-term severity (P_{st}), and the long-term severity (P_{lt}). These values represent the level of annoyance for the human eye due to flicker.

III. METHODOLOGY

This section presents the methodology for extracting the amplitudes and frequencies of the modulating waveform that causes flicker. The experiment is performed in a PV plant, and the methodology proposes a model to correlate flicker with some external parameters like irradiance and cell temperature. Fig. 1 depicts the method composed of three stages: envelope estimation, flicker parameter extraction, and correlation with external factors. The next signals are required to

apply this method: sun irradiance (*Irr*), cell temperature (*T*), the DC current (*Idc*) and voltage (*Vdc*) delivered by the PV modules, and the AC voltage (*Vac*) provided by the solar inverter. A proprietary data acquisition system (DAS) with an integrated data logger is developed for acquiring and collecting data from the PV installation.

Once data are collected, the flicker analysis is performed. The first stage estimates the envelope (*En*) of the *Vac* signal, generated by the solar inverter, using the Hilbert transform, [40]. This envelope considers any fluctuation present on the voltage signal, regardless of the source, and makes possible to assess the flicker due to a specific load, harmonic and inter harmonic components, and variation on the weather conditions, among others.

Since flicker is characterized by frequencies lower than the fundamental frequency, decimation is carried out on the envelope. This works as a low-pass filter and reduces the bandwidth of the signal, which is an advantage for the next stages because it simplifies the identification of frequencies lower than the fundamental frequency. Then, the sampling frequency is reduced from 8000 Hz to 128 Hz for obtaining the decimated envelope (*dEn*).

In the next stage, the flicker parameters are extracted in two steps after subtracting the mean value of the envelope (*dEn*) to eliminate any offset: firstly, the flicker frequencies are estimated, and secondly, their amplitude is measured (*Afl*). A MUSIC algorithm, with order 4, is used to estimate the flicker frequencies. MUSIC permits to identify, with a high-resolution, any frequency and their time evolution [41]. Notice that with this methodology, flicker is not considered constant with time. As MUSIC is not efficient at estimating amplitude, the DWT is used for this purpose and separates the envelope into several modes of different bandwidths. Since the modulating signal can contain more than one frequency, this decomposition allows measuring the amplitude of each flicker component present on the signal. The mother wavelet used is a Daubechies 12 and the levels of decomposition are set to 8. Finally, it is examined how the weather conditions affect the flicker by doing a correlation to external factors.

In the first step of this correlation analysis, two linear regressions are carried to find any relationship between *Irr*, *T*, *Vdc,* and *Idc*. The first one considers *Irr* and *T* as the explanatory variables and *Idc* as the dependent variable. The second one considers *Irr*, *T* and *Idc* as the explanatory variables and *Vdc* as the dependent one. The linear regression also permits to know the percentage of the dependent variable that can be described with the explanatory variables. This allows quantifying how the weather conditions affect the generation of the PV panel. The approach is performed this way due to the operating principle of PV cells, where the current delivered depends on the weather conditions, but the voltage may depend not only on the weather conditions but also on the generated current. Then, another linear regression is carried out to determine how *Vdc* and *Idc* are related to the flicker amplitude. Since the DC values are used to explain flicker, which occurs on the AC signal, it can be inferred that the percentage of the dependent variable that cannot be described by the explanatory variables is due to something related with the process of transforming DC into AC. Thus, it can be proved that the solar inverter directly affects the existence of flicker. Additionally, it is demonstrated that weather conditions are related to *Vdc* and *Idc*, and this last linear regression can provide information of the level of affection of weather conditions on flicker amplitude.

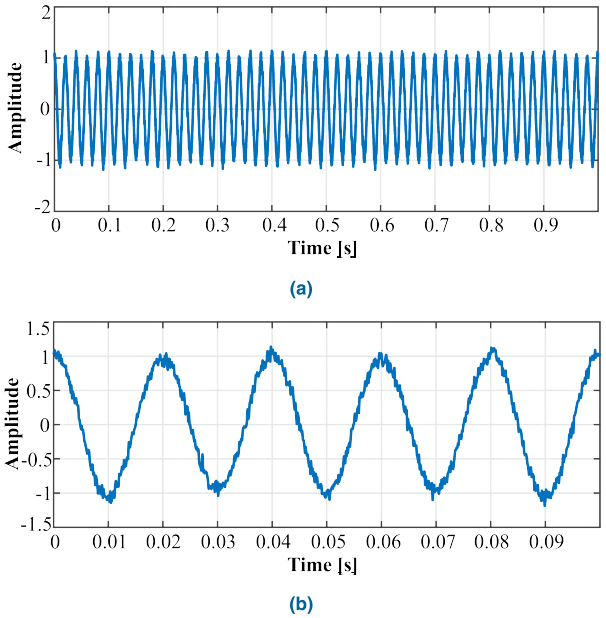

FIGURE 2. Synthetic signal with two flicker components and Gaussian noise; (a) 1 second detail, and (b) 0.1 second detail.

IV. VALIDATION OF THE PROPOSED METHODOLOGY

In this section, the proposed methodology is used to extract the parameters of flicker from two signals: one synthetic signal generated using (1), and a flicker waveform from the National Physical Laboratory (NPL) of the United Kingdom for calibration.

A. SYNTHETIC SIGNAL

Equation (1) is slightly modified adding Gaussian white noise to obtain a synthetic signal:

$$X_{fl}(t) = A \cdot [1 + \delta_a(t)] \cdot [cos(2\pi f_0 t + \theta)] + \eta_G \qquad (4)$$

where η_G represents the Gaussian white noise. This will permit to test the methodology with signals with a low signal-to-noise ratio (SNR). The SNR of the generated synthetic signal is 25 *dB*. The rest of parameters of (4) are: $A = 1$, $f_0 = 50\ Hz$, and $\theta = 0$. The function $\delta_a(t)$ is defined by (3) considering the next parameters: $n = 2$, $A_{fl} = [\,0.03\ 0.015\,]$, $f_{fl} = [\,22\ 10\,]\ Hz$, and $\theta_{fl} = [\,0\ 0\,]$. The duration of the signal is 10 minutes. Fig. 2(a) presents 1 second of the signal, where some amplitude variations are observable. However, the existence of noise introduces some other deformations on the waveform, which can be observed in detail in Fig. 2(b).

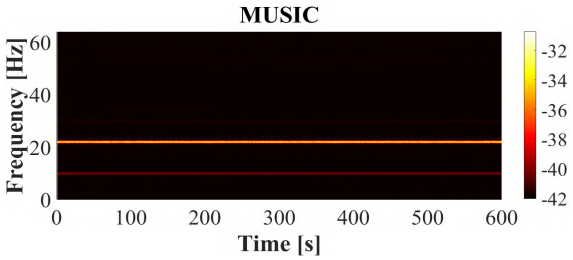

FIGURE 3. Estimation of the frequency components of flicker on the synthetic signal with two flicker components and Gaussian noise.

Fig. 3 shows the result of applying MUSIC to the envelope of the signal. There are two well-identified frequency components that correspond to the 22 and 10 Hz modulating signals used on the synthetic signal. Although MUSIC does not calculate signal amplitude reliably, it can be observed in Fig. 3 that the algorithm detects correctly that the energy of the 22 Hz component is larger than the one from the10 Hz component. Two additional components appear around 30 and 35 Hz. These components should not be present on the frequency estimation and they are a detrimental effect due to the noise. However, as their energy is very low, they can be ignored.

Fig. 4 shows the decomposition of the envelope performed with the DWT. Two modes are identified with clarify: one in the 16-8 Hz bandwidth (corresponding to the 10 Hz flicker component), and another one in the 32-16 Hz bandwidth (which represents the 22 Hz flicker component). Thus, it is demonstrated that the proposed methodology can identify correctly the two flicker signals, even in the presence of noise.

B. FLICKER WAVEFORM USED IN NPL (UK) FOR CALIBRATION

The National Physical Laboratory (NPL) is the entity in charge of the metrology and standards in the UK and they proposed a reference waveform used for flicker calibration [42]. The parameters selected for validation following the NPL recommendation are: flicker frequency 33.33 Hz and DV/V = 2.4. These parameters along $\theta_{fl} = 0$ are introduced in (3) to obtain the function $\delta_a(t)$. The rest of parameters take the following values: $A = 1, f_0 = 50\ Hz$, and $\theta = 0$. The resulting signal and its envelope are shown in Fig. 5.

MUSIC identifies correctly one frequency component (see Fig. 6), which appears around the value of 33.33 Hz, but the exact value reported by the algorithm is 33.375 Hz. This error is explained by the frequency resolution of the algorithm. A closer result to the real value can be obtained by modifying the time window, but this would compromise the time resolution.

If only one frequency component is present on the flicker signal, the amplitude can be obtained directly from the envelope to save processing time. Finally, the real amplitude and frequency values, along with the values delivered by the methodology and the error for the two synthetic signals, are summarized in Table 1. The error on the frequency estimation

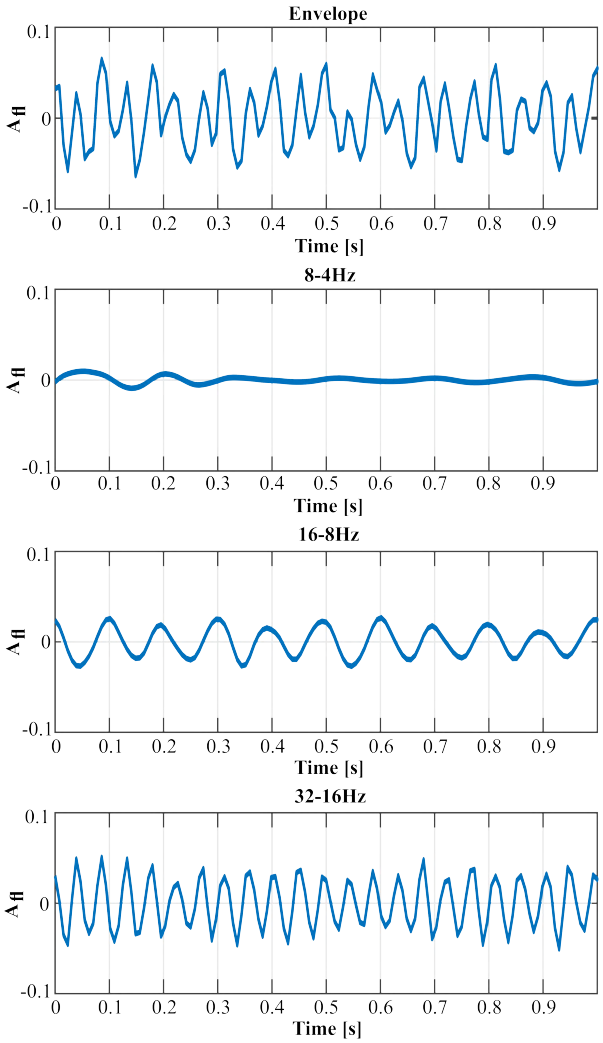

FIGURE 4. Amplitude estimation of the signal with two flicker components and Gaussian noise using DWT.

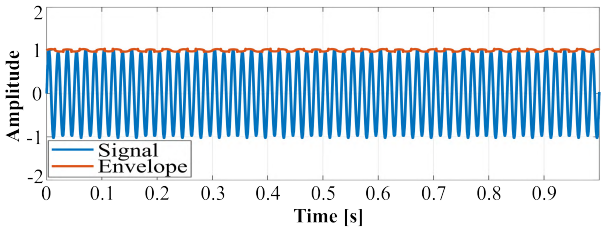

FIGURE 5. Waveform used in NPL for calibration and its envelope.

is very low, which is one of the strengths of this methodology. The amplitude errors are higher than frequency errors, but they are in a reasonable range.

V. EXPERIMENTAL SETUP

The experiment is performed at a 20 MW photovoltaic generation plant, located in central Spain. The plant is organized in independent branches of 100 kW each. A proprietary DAS is used for acquiring and collecting data from the photovoltaic installation. Fig. 7 depicts a general diagram of a

TABLE 1. Error on the estimation of the parameters of flicker.

Signal		Frequency (Hz)		Error (%)	Amplitude (p.u.)		Error (%)
		Real	Measure		Real	Measure	
Synthetic signal	Component 1	10	10	0	0.015	0.01469	2.1
	Component 2	22	22	0	0.03	0.02767	7.8
NPL Waveform	Component 1	33.33	33.375	0.135	0.024	0.02485	3.5

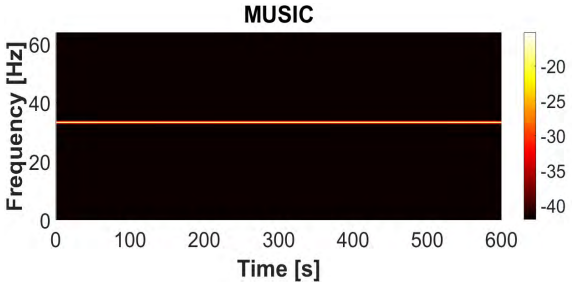

FIGURE 6. Flicker frequency estimation on the waveform used in NPL for calibration.

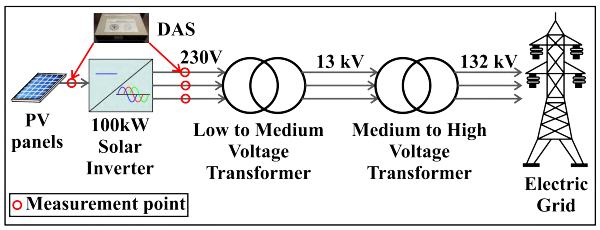

FIGURE 7. Diagram of one photovoltaic generation branch.

single branch of the generation plant and the location of the measurement instruments.

A. DESCRIPTION OF THE GENERATION NETWORK

Measurements are performed in two branches because two different solar inverters are used in the plant; in this way, it would be possible to study if the type of solar inverter affects the flicker levels. The two solar inverters used in this work are a Solarmax 100c [43] and an Ingecon Sun 100 [44]. The measurement points are marked with red circles in Fig. 7 to have a clearer idea of the location of the DAS.

B. DATA ACQUISITION SYSTEM

An FPGA-based DAS is developed for acquiring and collecting data from the photovoltaic installation. The designed DAS is able to acquire data from seven simultaneous channels at 8000 samples per second (SPS) with a 16-bit resolution. The equipment can store all the waveforms of voltage and current signals during an extended time using a standard micro SD card of 128 GB, which can be replaced when it is full, extending the storage capacity. On the DC side, only two channels of the DAS are used: one for the voltage and another for the current. The DC voltage level is around 600 V and the current about 250 A. This DAS is conditioned to measure voltages up to 1000 V and the current is acquired using an effect hall clamp whose output voltage is in the ±4 V range. This sensor is the HOP 500-SB/SP1 by LEM [45]. On the AC side, six channels of the DAS are required to measure the voltage (230 Vrms) and current of the three phases (5 Arms). The currents are measured in the secondary of a current transformer (200/5 ratio) using the SCT-013-010 sensors by YHDC [46].

VI. RESULTS AND DISCUSSION

A. FLICKER ESTIMATION

The proposed methodology is applied to real signals from a photovoltaic plant. The signals are selected from three days with different conditions regarding solar irradiance and temperature: (i) The first day is a sunny day (Fig. 8); (ii) The second day presents some clouds at certain moments, which affects the solar irradiance (Fig. 9); (iii) The third day is a cloudy and stormy day, where the irradiance is very low and presents sudden variations along the day (Fig. 10). Therefore, the irradiance and cell temperature profiles of the three days are different and show abrupt variations when clouds are present in the sky (see Fig. 8(a), 8(b), 9(a), 9(b), 10(a) and 10(b)). The cell temperature profile depends highly on the irradiance. Fig. 8(c), 8(d), 9(c), 9(d), 10(c) and 10(d) present the flicker calculated for each day and the two inverters considered. The frequency of the flicker is averaged every 60 seconds for the sake of consistency with the irradiance data, which were collected on a minute basis. The amplitude of the flicker is represented using a color scale, with yellow for the highest value and blue for the lowest one, and it is obtained using the DWT. With this technique, the signal is decomposed into different modes, which are selected depending on the value of the frequency. Then, the amplitude is assigned to that frequency and time with a correct color according to the color scale selected.

It is worth noticing that both inverters present very different flicker levels, despite being in the same location. While the Ingecon Sun 100 inverter presents various flicker components (see Fig. 9(c)), the Solarmax 100c inverter barely shows a component in frequencies near to zero Hz and with amplitudes that are almost negligible (Fig. 9(d)). It is also noticeable that there is a correspondence between the highest values of the flicker amplitude and irradiance and cell temperature (Fig. 8(c)). During the night, when the PV cells and the solar inverters are not operating, there are no flicker components.

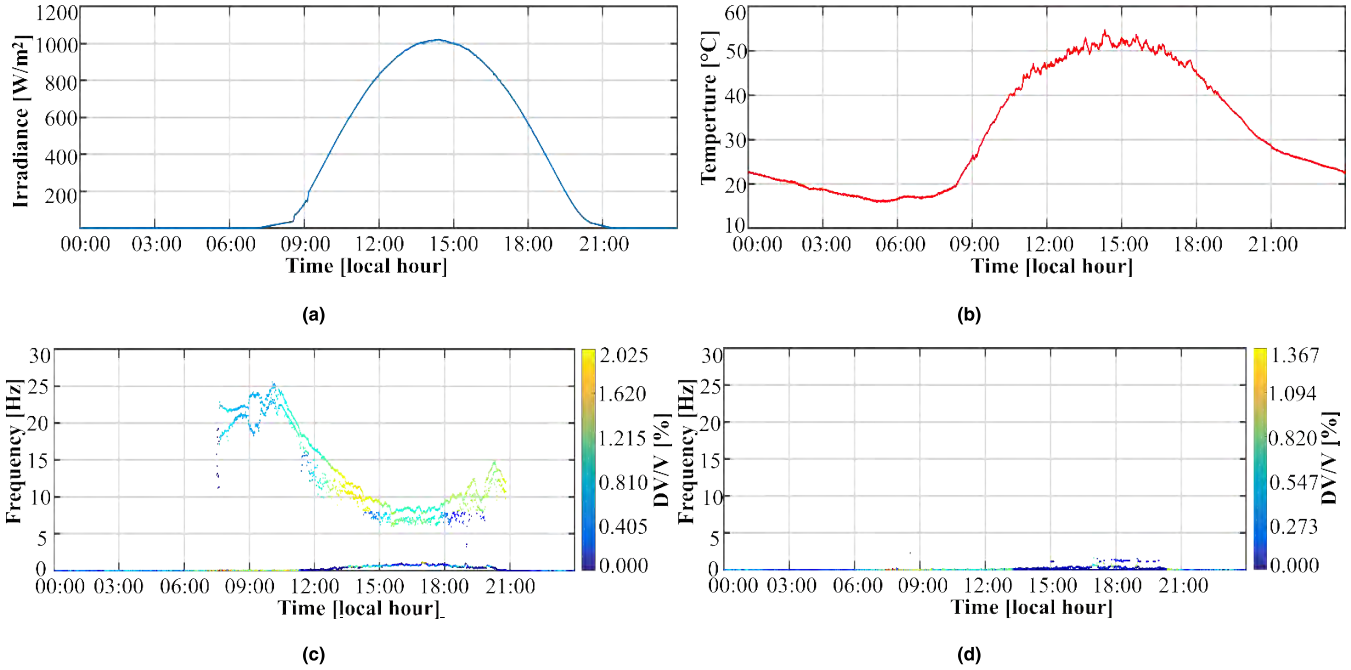

FIGURE 8. First day (a) Irradiance, (b) cell temperature, (c) flicker estimation on Ingecon sun 100 inverter, and (d) flicker estimation on Solarmax 100c inverter.

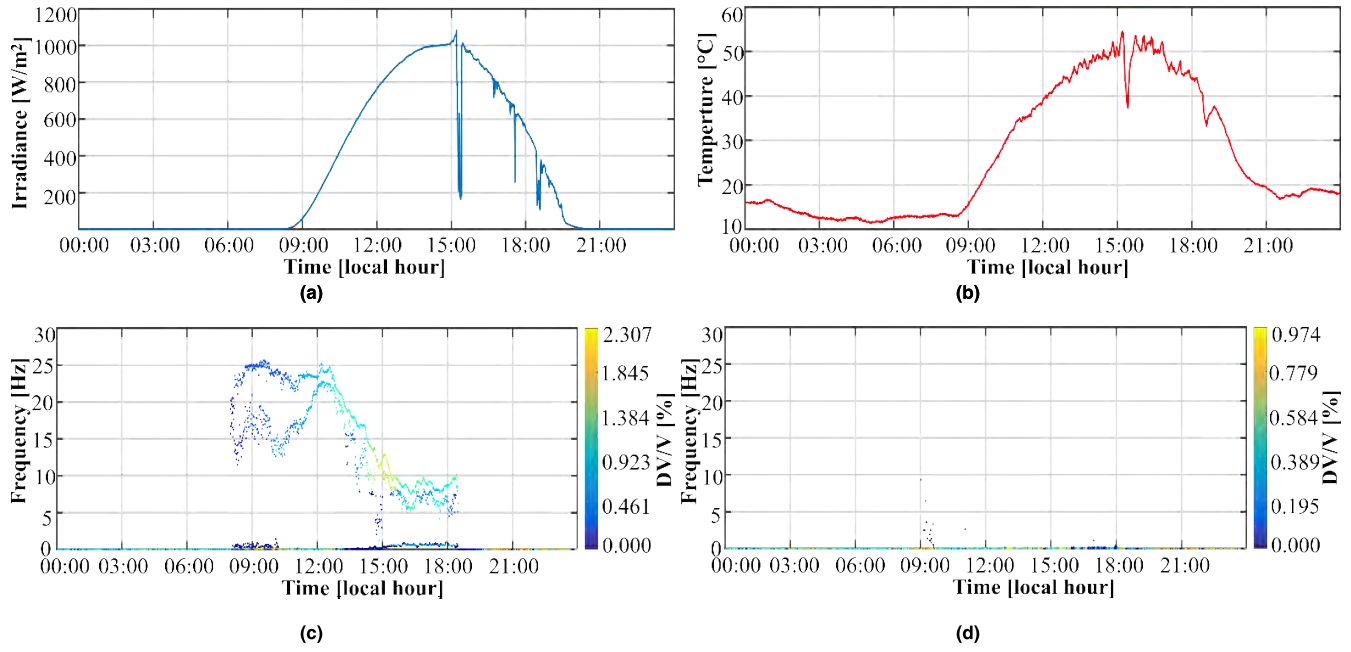

FIGURE 9. Second day (a) Irradiance, (b) cell temperature, (c) flicker estimation on Ingecon sun 100 inverter, and (d) flicker estimation on Solarmax 100c inverter.

Hence, the existence of flicker during the day is due to the PV generation process.

Fig. 8(c) illustrates another important result as it displays three well-defined flicker components whose frequency is not constant with time. The methodologies reported so far consider that flicker is constant for the entire time interval of analysis. The results obtained with the proposed methodology in this work prove that flicker is a phenomenon that is not necessarily stationary.

Therefore, these results from the analysis of the three different days suggest that the existence of flicker in PV generation is related to weather conditions as well as to the solar inverter model. Two different inverters were tested during three separate days and at the same location.

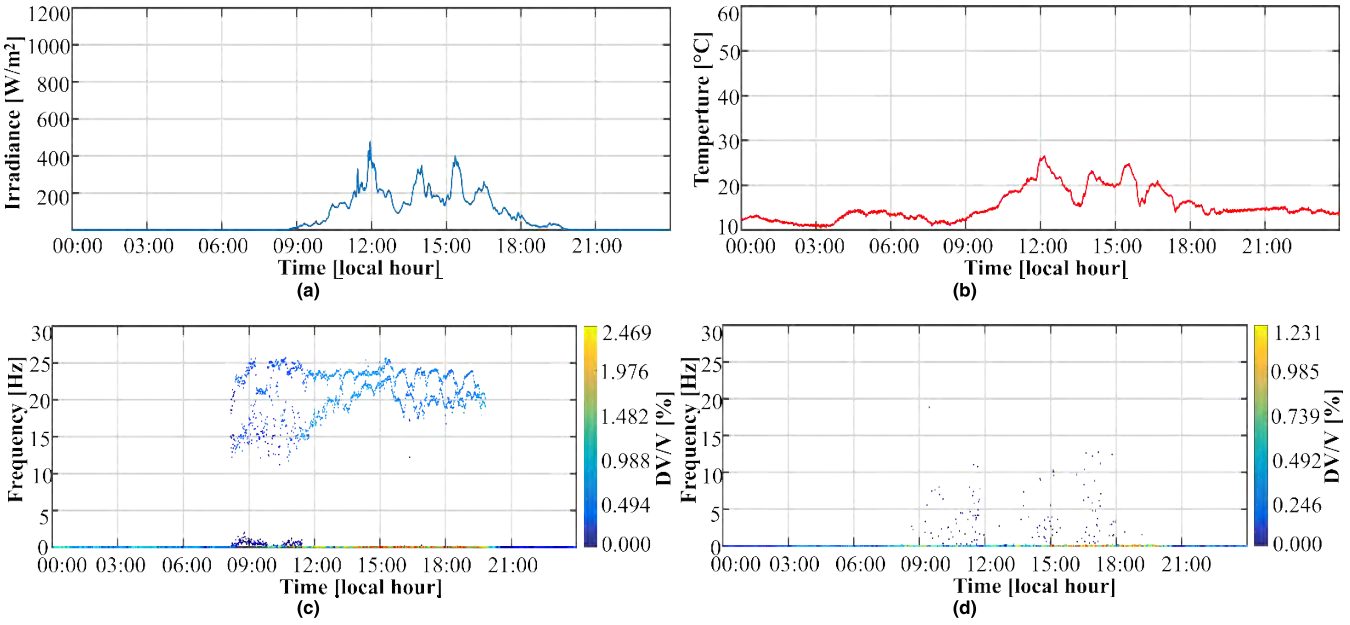

FIGURE 10. Third day (a) Irradiance, (b) cell temperature, (c) flicker estimation on Ingecon sun 100 inverter, and (d) flicker estimation on Solarmax 100c inverter.

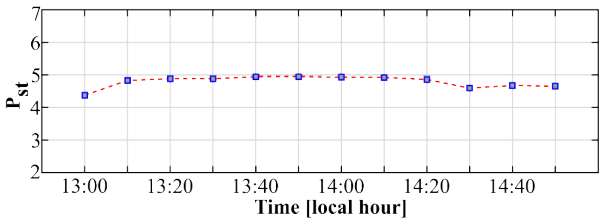

FIGURE 11. P_{st} for a two-hour period of the first day of analysis.

The level of flicker they presented was very different. Therefore, the principle of operation of the solar inverter could also be a source of the flicker.

B. COMPARATIVE WITH STANDARD IEC 61000-4-15

Standard IEC 61000-4-15 establishes the admissible levels of flicker and defines a methodology for measuring these levels. The standard uses two values for describing the severity of flicker in voltage signals: the short-term severity (P_{st}) that is measured over a period of 10 minutes, and the long-term severity (P_{lt}) which is calculated from a sequence of 12 consecutive P_{st} values. A flickermeter based on the standard is designed for obtaining the P_{st} values for the period comprised between the 13:00 and the 15:00 hours of the first day of analysis. Only the signal from Ingecon Sun 100 inverter is used because is the one that presents flicker components. The P_{st} values are presented in Fig. 11. The blue squares in Fig. 11 correspond to every P_{st} value, whereas the dotted red line represent the flicker tendency. This figure shows that the flicker severity of the signal is much higher than the permissive value stated by the standard, which is 1.00. It is also observed that the P_{st} values present a tendency very similar to the one presented by the flicker amplitude in Fig. 8(c), i.e., the flicker level starts raising and reaches a top value near the 14:00 hours, then the flicker level starts decaying. However, the P_{st} values do not provide information regard the frequency of the flicker component. Moreover, the standard does not consider the existence of more than one flicker component. Additionally, the standard considers a 10-minute period for the estimation of every P_{st} value and some rapid variations on the flicker levels may be missed by this situation. It is important to mention that the standard delivers statistical values that represent the level of annoyance due to flicker, whereas the methodology described in this work provides information on the parameters that describe flicker and their behavior. In this sense, the methodology proposed in this work could also be considered as a compliment to the standard in order to provide more information about the flicker behavior along the day, and the time window may be modified if there is a situation that requires it.

C. RELATION OF FLICKER WITH EXTERNAL FACTORS

A linear regression model is used to quantify and explain how the weather conditions are related to the appearance of flicker on PV installations. First, two linear regressions are carried out: the first for identifying the relationship between weather conditions and *Vdc,* and the second between weather conditions, *Idc* and *Vdc*. This analysis is performed for the same three days presented before. As the Ingecom Sun 100 presented higher levels of flicker, this study is applied only to it. The linear regression model used to explain *Idc* is described by (5):

$$Idc = Intercept + c_1 Irr + c_2 T \tag{5}$$

TABLE 2. Linear regression results for weather conditions and *Idc* for day one.

Variable	*Coefficients*	*Standard Error*	*t Statistic*	*p-Value*
Intercept	14.423	0.713	20.216	$3.552\text{x}10^{-80}$
Irradiance	0.231	$1.069\text{x}10^{-3}$	216.450	0
Temperature	-0.591	$3.187\text{x}10^{-2}$	-18.531	$6.569\text{x}10^{-69}$
Adjusted R-Squared: 0.997				

TABLE 3. Linear regression results for weather conditions, *Idc* and *Vdc* for day one.

Variable	*Coefficients*	*Standard Error*	*t Statistic*	*p-Value*
Intercept	-290.760	18.782	-15.481	$4.203\text{x}10^{-50}$
Irradiance	-8.887	0.530	-16.761	$1.022\text{x}10^{-57}$
Temperature	14.723	0.839	17.549	$1.324\text{x}10^{-62}$
Current	57.502	2.522	22.799	$2.017\text{x}10^{-98}$
*Irradiance*Temperature*	0.264	$1.335\text{x}10^{-2}$	19.773	$3.872\text{x}10^{-77}$
*Irradiance*Current*	$4.695\text{x}10^{-3}$	$5.244\text{x}10^{-4}$	8.953	$1.048\text{x}10^{-18}$
*Temperature*Current*	-1.639	$7.284\text{x}10^{-2}$	-22.502	$2.896\text{x}10^{-96}$
Adjusted R-Squared: 0.836				

The values of *Intercept*, c_1 and c_2 are the coefficients estimated through the linear regression. Table 2 summarizes the most important statistical values delivered by the linear regression process applied to the data of the first day analyzed.

The relevance of one variable on the explanation of the response variable is ensured by a *p-value* of the *t statistic* equal to zero or very close to it. These values are very low in Table 2 so, the irradiance and cell temperature have a significant impact on the *Idc* (response variable). The *Adjusted R-Squared* value defines how much of the response variable can be represented by the explanatory variables. Then, in this case, the irradiance and cell temperature can explain 99.7% of the behavior of *Idc*. The linear regression model to study the *Vdc* is as follows described by (6):

$$Vdc = Intercept + c_1 Irr + c_2 T + c_3 Idc + c_4(Irr)(T) + c_5(Irr)(Idc) + c_6(T)(Idc) \quad (6)$$

Where $Intercept, c_1, c_2, c_3, c_4, c_5$ and c_6 are the coefficients delivered by the linear regression process. The irradiance, cell temperature and *Idc* are now the explanatory variables. This model also considers their interactions. The results are in Table 3.

It is observed that the *p-Value* of all variables is very close to zero. However, as the coefficient of the interaction between irradiance and current is very low, the interaction between these variables is not relevant for the description of the response variable. The value of the *Adjusted R-Squared* says that only around an 83.6% of the *Vdc* is explained by the mathematical model of (6). Results from both regression models show that there is a strong relationship between the weather conditions and the current and voltage generated. Moreover, they quantify the level of affection of each variable, which is one of the most important contributions of this work.

These linear regression models were also applied to the data of the other two days getting similar results.

Since it has been proved that *Idc* and *Vdc* are related to the weather conditions, by proving that they are related to flicker it will be inferred that flicker is related to the weather conditions. Then, another linear regression is carried out, using *Idc* and *Vdc* as explanatory variables, and being the flicker amplitude as the response variable. This analysis is applied to every flicker frequency component detected, which will be named as the bottom component (the component with the lowest frequencies), middle component, and top component (the component with the highest frequencies). This linear regression uses a quadratic model like the one in (7).

$$A_{fl} = Intercept + c_1 Idc + c_2 Vdc + c_3(Idc)(Vdc) + c_4 Idc^2 + c_5 Vdc^2 \quad (7)$$

Where A_{fl} is the flicker amplitude, and $Intercept, c_1, c_2, c_3, c_4$ and c_5 are the coefficients delivered by the linear regression. This model also contains interactions and squared terms. This model is the one that best fit to the behavior of the flicker components. Tables 4, 5 and 6 summarize the results for the three flicker components of day one.

The results from tables 4, 5 and 6 show that all variables are highly correlated to the three flicker components. All *p-values* are close to zero, and the *Adjusted R-Squared* values are high. This means that the explanatory variables can explain the behavior of flicker almost completely. Although the variables explain a significant part of the phenomenon, they are not the only ones involved in its description. The other element not present in the analysis is the solar inverter, so it can be assumed that the operation of the inverter is the missing variable required for a better description of flicker. A similar analysis is also performed to the data from the third day (tables 7, 8 and 9).

TABLE 4. Linear regression results for *Idc, Vdc* and flicker bottom component for day one.

Variable	*Coefficients*	*Standard Error*	*t Statistic*	*p-Value*
Intercept	-0.269	$6.069\text{x}10^{-3}$	-44.386	$1.752\text{x}10^{-271}$
Current	0.176	$2.843\text{x}10^{-3}$	61.979	0
Voltage	$2.118\text{x}10^{-3}$	$2.146\text{x}10^{-4}$	9.867	$2.919\text{x}10^{-22}$
*Current*Voltage*	$-3.201\text{x}10^{-4}$	$5.388\text{x}10^{-6}$	-59.415	0
Current^2	$-1.464\text{x}10^{-4}$	$2.426\text{x}10^{-6}$	-60.353	0
Voltage^2	$-4.537\text{x}10^{-6}$	$4.877\text{x}10^{-7}$	-9.303	$4.909\text{x}10^{-20}$
Adjusted R-Squared: 0.870				

TABLE 5. Linear regression results for *Idc, Vdc* and flicker middle component for day one.

Variable	*Coefficients*	*Standard Error*	*t Statistic*	*p-Value*
Intercept	4.379	0.135	32.477	$6.814\text{x}10^{-174}$
Current	-2.743	$6.316\text{x}10^{-2}$	-43.420	$1.258\text{x}10^{-263}$
Voltage	$1.540\text{x}10^{-2}$	$4.769\text{x}10^{-3}$	3.230	$1.265\text{x}10^{-3}$
*Current*Voltage*	$5.018\text{x}10^{-3}$	$1.197\text{x}10^{-4}$	41.918	$2.350\text{x}10^{-251}$
Current^2	$2.197\text{x}10^{-3}$	$5.392\text{x}10^{-5}$	40.757	$7.674\text{x}10^{-242}$
Voltage^2	$4.963\text{x}10^{-5}$	$1.084\text{x}10^{-5}$	4.580	$5.049\text{x}10^{-6}$
Adjusted R-Squared: 0.895				

TABLE 6. Linear regression results for *Idc, Vdc* and flicker top component for day one.

Variable	*Coefficients*	*Standard Error*	*t Statistic*	*p-Value*
Intercept	4.633	0.142	32.635	$3.523\text{x}10^{-175}$
Current	-2.864	$6.649\text{x}10^{-2}$	-43.066	$9.749\text{x}10^{-261}$
Voltage	$2.236\text{x}10^{-2}$	$5.020\text{x}10^{-3}$	4.453	$9.132\text{x}10^{-6}$
*Current*Voltage*	$5.233\text{x}10^{-3}$	$1.260\text{x}10^{-4}$	41.516	$4.641\text{x}10^{-248}$
Current^2	$2.306\text{x}10^{-3}$	$5.676\text{x}10^{-5}$	40.631	$8.283\text{x}10^{-241}$
Voltage^2	$4.609\text{x}10^{-5}$	$1.141\text{x}10^{-5}$	4.039	$5.630\text{x}10^{-5}$
Adjusted R-Squared: 0.908				

TABLE 7. Linear regression results for *Idc, Vdc* and flicker bottom component for day three.

Variable	*Coefficients*	*Standard Error*	*t Statistic*	*p-Value*
Intercept	$7.400\text{x}10^{-2}$	$2.399\text{x}10^{-2}$	3.084	$2.081\text{x}10^{-3}$
Current	$-3.763\text{x}10^{-2}$	$1.382\text{x}10^{-2}$	-2.723	$6.551\text{x}10^{-3}$
Voltage	$7.299\text{x}10^{-4}$	$4.494\text{x}10^{-4}$	1.624	0.105
*Current*Voltage*	$4.108\text{x}10^{-5}$	$2.718\text{x}10^{-5}$	1.511	0.131
Current^2	$1.545\text{x}10^{-4}$	$2.798\text{x}10^{-5}$	5.521	$4.001\text{x}10^{-8}$
Voltage^2	$1.482\text{x}10^{-7}$	$1.143\text{x}10^{-6}$	0.129	0.897
Adjusted R-Squared: 0.168				

The value of the *Adjusted R-Squared* in Table 7 is very low, which suggests that the bottom frequency component is not related to environmental factors like irradiance and cell temperature. This result is corroborated by Fig. 11(c), 12(c) and 13(c), where it is noticeable that the bottom frequency component presents values of amplitude different from zero even during the night. During the night, the solar inverter remains connected to the grid, but it is not operating, so every frequency component that presents amplitudes different from zero cannot be related to PV generation.

Nevertheless, the middle and top frequency components present very low *p-Value* and *Adjust R-Squared* values high enough to prove that these frequency components are related to irradiance and cell temperature. It is important to mention that some coefficients are very low. There are also some *p-Values*, like the one of the variable named *Current^2* in Table 9, that are not as close to zero as they should be to ensure that this variable is significant for the explanation of the response variable. These results corroborate that, although flicker is related to irradiance and cell temperature, there are other variables that affect the behavior of flicker. Additionally, it can be said that weather conditions explain between the 70% or 80% of the flicker behavior. The missing 20% to 30% can be attributed to the DC to AC conversion stage,

TABLE 8. Linear regression results for *Idc, Vdc* and flicker middle component for day three.

Variable	*Coefficients*	*Standard Error*	*t Statistic*	*p-Value*
Intercept	-1.113	0.527	-2.111	$3.496\text{x}10^{-2}$
Current	1.539	0.304	5.066	$4.591\text{x}10^{-7}$
Voltage	$7.164\text{x}10^{-2}$	$9.879\text{x}10^{-3}$	7.252	$6.719\text{x}10^{-13}$
*Current*Voltage*	$-2.727\text{x}10^{-3}$	$5.975\text{x}10^{-4}$	-4.565	$5.431\text{x}10^{-6}$
Current^2	$-1.022\text{x}10^{-3}$	$6.150\text{x}10^{-4}$	-1.661	$9.692\text{x}10^{-2}$
Voltage^2	$-7.844\text{x}10^{-5}$	$2.513\text{x}10^{-5}$	-3.121	$1.837\text{x}10^{-3}$
Adjusted R-Squared: 0.819				

TABLE 9. Linear regression results for *Idc, Vdc* and flicker top component for day three.

Variable	*Coefficients*	*Standard Error*	*t Statistic*	*p-Value*
Intercept	-1.623	0.577	-2.814	$4.967\text{x}10^{-3}$
Current	2.019	0.332	6.076	$1.581\text{x}10^{-9}$
Voltage	$7.781\text{x}10^{-2}$	$1.081\text{x}10^{-2}$	7.200	$9.654\text{x}10^{-13}$
*Current*Voltage*	$-3.784\text{x}10^{-3}$	$6.536\text{x}10^{-4}$	-5.789	$8.664\text{x}10^{-9}$
Current^2	$-2.338\text{x}10^{-4}$	$6.728\text{x}10^{-4}$	-0.348	0.728
Voltage^2	$-6.662\text{x}10^{-5}$	$2.749\text{x}10^{-5}$	-2.423	$1.550\text{x}10^{-2}$
Adjusted R-Squared: 0.856				

because the solar inverters used for this purpose contain a large number of power electronic devices that represent non-linear loads for the electric grid. Moreover, two different solar inverters are tested in this study, and one of them introduces flicker whereas the second does not introduce flicker. Then, the solar inverter operation principle can also be encompassed in this 20% to 30% that cannot be explained by the environmental conditions. Finally, these results can give an explanation to the rise and drop in flicker amplitude.as they show that a rising in temperature and sun irradiance has a high probability to result in a flicker amplitude rising. Moreover, it is aforementioned that flicker is related with the existence of harmonics and interharmonics in the voltage signal; thus, it can be inferred that fluctuations on weather conditions modify the spectral content of the voltage signal affecting the flicker behavior.

VII. CONCLUSIONS

This work proposes a methodology that proves to be effective for the extraction of the parameters of flicker. It uses two well-studied techniques: MUSIC and DWT. MUSIC delivers a high-resolution estimation of the frequency, but it cannot estimate the energy of a signal accurately, so it is estimated using the DWT. Thus, these two techniques are combined to take advantage of their strengths and to obtain a useful tool for frequency and amplitude estimation. The results prove that voltage signals can contain different flicker frequencies, and this methodology permits to identify and analyze them separately. Another capability of this method is its ability to study flicker components that are not stationary, detecting their instant variations in frequency and amplitude. The methodology is applied to real signals from a 20MW PV generation plant. The signals correspond to three days of production with different weather conditions. Results demonstrate that PV generation itself introduces flicker into the grid because only during the day some frequency components that modulate the voltage signal appear.

It can also be inferred that the weather conditions affect the characteristics of the flicker. Moreover, it is demonstrated that for the same location, one solar inverter generates a flicker signal and the other one does not. Thus, it can be said that the type of solar inverter is also a source of flicker.

Notwithstanding, one of the aims of this work consist in performing not only a qualitative but a quantitative analysis of the influence of weather conditions and solar inverter on the existence of flicker in PV generation process. While most of the works consider only the influence of irradiance in the PV generation process, this work considers irradiance and cell temperature. In this sense, the linear regression analysis proves that solar irradiance and cell temperature can explain by themselves more than the 97% of the behavior of the DC current and around the 85% of the DC voltage. Additionally, the DC voltage and current can explain around a 70% or 80% of the flicker present on the PV generation process. Since the DC variables are highly related to weather conditions, it is safe to ensure that flicker is related to weather conditions to the same extent. Despite the *p-Value* delivered by these last linear regression models prove that flicker is related to weather conditions, some of the coefficients make the contribution of an explanatory variable negligible. The existence of a variable highly correlated with a phenomenon but which contribution is insignificant, is not a common situation. This situation, together with the fact that the explanatory variables cannot describe 100% of the flicker behavior, allows to assert that solar irradiance and cell temperature are not the only variables that describe the flicker existence in

PV generation. Results prove that weather conditions are related to DC generation process. Since PV generation is performed in two stages: DC generation, and DC to AC conversion, it can be said that the percentage of the flicker that cannot be explained by weather conditions is due to the DC to AC conversion, i.e., the action of the solar inverter is directly correlated with flicker existence. It is important considering that international standards evaluate flicker based on the unsteadiness of lighting loads; however, this study focuses on the waveform resulting from the PV generation process. In this sense, the assessing of the output with any lighting load may deliver interesting results and it is left for further applications.

REFERENCES

[1] A. Hussain, S. M. Arif, and M. Aslam, "Emerging renewable and sustainable energy technologies: State of the art," *Renew. Sustain. Energy Rev.*, vol. 71, pp. 12–28, May 2017.

[2] D. Parra, M. Gillott, S. A. Norman, and G. S. Walker, "Optimum community energy storage system for PV energy time-shift," *Appl. Energy*, vol. 137, pp. 576–587, Jan. 2015.

[3] L. Hadjidemetriou, Y. Yang, E. Kyriakides, and F. Blaabjerg, "A synchronization scheme for single-phase grid-tied inverters under harmonic distortion and grid disturbances," *IEEE Trans. Power Electron.*, vol. 32, no. 4, pp. 2784–2793, Apr. 2016.

[4] Y. Du, D. D.-C. Lu, G. James, and D. J. Cornforth, "Modeling and analysis of current harmonic distortion from grid connected PV inverters under different operating conditions," *Sol. Energy*, vol. 94, pp. 182–194, Aug. 2013.

[5] D. D. C. Lu and Q. N. Nguyen, "A photovoltaic panel emulator using a buck-boost DC/DC converter and a low cost micro-controller," *Sol. Energy*, vol. 86, no. 5, pp. 1477–1484, 2012.

[6] M. Kopicka, M. Ptacek, and P. Toman, "Analysis of the power quality and the impact of photovoltaic power plant operation on low-voltage distribution network," in *Proc. Electr. Power Quality Supply Rel. Conf. (PQ)*, Rakvere, Estonia. Jun. 2014, pp. 99–102.

[7] G. de Oliveira e Silva and P. Hendrick, "Photovoltaic self-sufficiency of Belgian households using lithium-ion batteries, and its impact on the grid," *Appl. Energy*, vol. 195, pp. 786–799, Jun. 2017.

[8] *IEEE Recommended Practice for Measurement and Limits of Voltage Fluctuations and Associated Light Flicker on AC Power Systems*, IEEE Standard 1453-2004, The Institute of Electrial and Electronics Engineers, New York, NY, USA, Oct. 2004.

[9] B. Eidson and M. Halpin, "An evaluation of the extent of correlation between interharmonic and voltage fluctuation measurements," *IEEE Trans. Power Del.*, vol. 31, no. 2, pp. 753–760, Feb. 2016.

[10] G. Z. Peng, M. A. M. Radzi, H. Hizam, and N. I. A. Wahab, "A simple predictive method of critical flicker detection for human healthy precaution," *Math. Problems Eng.*, vol. 2015, pp. 1–10, Sep. 2015. [Online]. Available: http://dx.doi.org/10.1155/2015/871826

[11] S. R. Samantaray, P. D. Achlerkar, and M. S. Manikandan, "Variational mode decomposition and decision tree based detection and classification of powerquality disturbances in grid-connected distributed generation system," *IEEE Trans. Smart Grid*, to be published. [Online]. Available: http://dx.doi.org/10.1109/TSG.2016.2626469

[12] *Testing and Measurement Techniques—Flickermeter—Functional and Design Specifications*, IEC International Standard 61000-4-15, International Electrotechnical Commission, Geneva, Switzerland, 2010.

[13] A. Hooshyar, M. A. Azzouz, and E. F. El-Saadany, "Addressing IEC flickermeter deficiencies by digital filtration inside a sliding window," *IEEE Trans. Instrum. Meas.*, vol. 62, no. 9, pp. 2476–2491, Sep. 2013.

[14] J. Ruiz *et al.*, "Influence of the carrier phase on flicker measurement for rectangular voltage fluctuations," *IEEE Trans. Instrum. Meas.*, vol. 61, no. 3, pp. 629–635, Mar. 2012.

[15] L. Feola, R. Langella, and A. Testa, "A new frequency approach for light flicker evaluation in electric power systems," *EURASIP J. Adv. Signal Process.*, vol. 2015, no. 1, pp. 1–12, Dec. 2015.

[16] A. Hernandez, J. G. Mayordomo, R. Asensi, and L. F. Beites, "A new frequency domain approach for flicker evaluation of arc furnaces," *IEEE Trans. Power Del.*, vol. 18, no. 2, pp. 631–638, Apr. 2003.

[17] N. Köse and Ö. Salor, "New spectral decomposition based approach for flicker evaluation of electric arc furnaces," *IET Generat. Trans. Distrib.*, vol. 3, no. 4, pp. 393–411, 2009.

[18] G. W. Chang, C.-I. Chen, and Y.-L. Huang, "A digital implementation of flickermeter in the hybrid time and frequency domains," *IEEE Trans. Power Del.*, vol. 24, no. 3, pp. 1475–1482, Jul. 2009.

[19] T. Keppler, N. R. Watson, J. Arrillaga, and S. Chen, "Theoretical assessment of light flicker caused by sub- and interharmonic frequencies," *IEEE Trans. Power Del.*, vol. 18, no. 1, pp. 329–333, Jan. 2003.

[20] M. A. Rodriguez-Guerrero, R. Carranza-Lopez-Padilla, R. A. Osornio-Rios, and R. de J. Romero-Troncoso, "A novel methodology for modeling waveforms for power quality disturbance analysis," *Electr. Power Syst. Res.*, vol. 143, pp. 14–24, Feb. 2017.

[21] D. Camarena-Martinez, M. Valtierra-Rodriguez, C. A. Perez-Ramirez, J. P. Amezquita-Sanchez, R. de J. Romero-Troncoso, and A. Garcia-Perez, "Novel downsampling empirical mode decomposition approach for power quality analysis," *IEEE Trans. Ind. Electron.*, vol. 63, no. 4, pp. 2369–2378, Apr. 2016.

[22] M. Valtierra-Rodriguez, R. D. J. Romero-Troncoso, A. Garcia-Perez, D. Granados-Lieberman, and R. A. Osornio-Rios, "Reconfigurable instrument for neural-network-based power-quality monitoring in 3-phase power systems," *IET Generat. Trans. Distrib.*, vol. 7, no. 12, pp. 1498–1507, 2013.

[23] E. Balouji and O. Salor, "Digital realisation of the IEC flickermeter using root mean square of the voltage waveform," *IET Generat. Trans. Distrib.*, vol. 10, no. 7, pp. 1663–1670, 2016.

[24] X. Chen, Y. Hou, S. C. Tan, C. K. Lee, and S. Y. R. Hui, "Mitigating voltage and frequency fluctuation in microgrids using electric springs," *IEEE Trans. Smart Grid*, vol. 6, no. 2, pp. 508–515, Mar. 2015.

[25] S. K. Sharma, A. Chandra, M. Saad, S. Lefebvre, D. Asber, and L. Lenoir, "Voltage flicker mitigation employing smart loads with high penetration of renewable energy in distribution systems," *IEEE Trans. Sustain. Energy*, vol. 8, no. 1, pp. 414–424, Jan. 2017.

[26] H. Samet and M. A. Jarrahi, "A comparison between SVC and STATCOM in flicker mitigation of electric arc furnace using practical recorded data," in *Proc. 30th Power Syst. Conf. (PSC)*, Tehran, Iran. Nov. 2015, pp. 300–304.

[27] M. Morati, D. Girod, F. Terrien, V. Peron, P. Poure, and S. Saadate, "Industrial 100-MVA EAF voltage flicker mitigation using VSC-based STATCOM with improved performance," *IEEE Trans. Power Del.*, vol. 31, no. 6, pp. 2494–2501, Dec. 2016.

[28] M. J. Ferdous, Y. Arafat, and M. A. Azam, "Flicker level mitigation of weak grid connected wind turbine with DFIG by injecting optimum reactive power using STATCOM," in *Proc. Int. Conf. Inform., Electron. Vis. (ICIEV)*, Dhaka, Bangladesh, May 2013, pp. 1–5.

[29] M. Karami, H. A. Shayanfar, A. G. Tapeh, and S. Bandari, "Learning techniques to train neural networks as a state selector in direct power control of DSTATCOM for voltage flicker mitigation," in *Proc. Int. Conf. Inf. Technol., New Generat. (ITNG)*, Las Vegas, NV, USA, Apr. 2008.

[30] B. Singh and S. R. Arya, "Back-propagation control algorithm for power quality improvement using DSTATCOM," *IEEE Trans. Ind. Electron.*, vol. 61, no. 3, pp. 1204–1212, Mar. 2009.

[31] M. Ebad and W. M. Grady, "An approach for assessing high-penetration PV impact on distribution feeders," *Electr. Power Syst. Res.*, vol. 133, pp. 347–354, Apr. 2016.

[32] P. Mohammadi and S. Mehraeen, "Challenges of PV integration in low-voltage secondary networks," *IEEE Trans. Power Del.*, vol. 32, no. 1, pp. 525–535, Feb. 2017.

[33] A. Chidurala, T. Saha, and N. Mithulananthan, "Field investigation of voltage quality issues in distribution network with PV penetration," in *Proc. IEEE PES Asia-Pacific Power Energy Eng. Conf. (APPEEC)*, Brisbane, QLD, Australia, Nov. 2015, pp. 1–5.

[34] P. Pakonen, A. Hilden, T. Suntio, and P. Verho, "Grid-connected PV power plant induced power quality problems—Experimental evidence," in *Proc. IEEE 18th Eur. Conf. Power Electron. Appl. (EPE ECCE Europe)*, Karlsruhe, Germany, Sep. 2016, pp. 1–10.

[35] J. C. Hernández, M. J. Ortega, J. De la Cruz, and D. Vera, "Guidelines for the technical assessment of harmonic, flicker and unbalance emission limits for PV-distributed generation," *Electr. Power Syst. Res.*, vol. 81, no. 7, pp. 1247–1257, 2011.

[36] R. Seguin, J. Woyak, D. Costyk, J. Hambrick, and B. Mather, "High-penetration PV integration handbook for distribution engineers," U.S. Dept. Energy, Nat. Renew. Energy Lab., Golden, CO, USA, Tech. Rep. NREL/TP-5D00-63114, 2016.

[37] D. Wei, H. Jingsheng, Z. Fei, and Z. Xiaolin, "A flicker assessment method for PV plants considering solar radiation condition," in *Proc. China Int. Conf. Electr. Distrib. (CICED)*, Xi'an, China, Aug. 2016, pp. 1–5.
[38] Z. Hanzelka and A. Bierí, "Harmonics interharmonics," Eur. Copper Inst. AGH Univ. Sci. Technol. Copper Develop. Assoc., Brussels, Belgium, Tech. Rep. 3.1.1, 2004.
[39] *IEEE Recommended Practice for Monitoring Electric Power Quality*, IEEE Standard 1159, Institute of Electrical and Electronic Engineers, Jun. 2009.
[40] D. Granados-Lieberman, M. Valtierra-Rodriguez, L. A. Morales-Hernandez, R. J. Romero-Troncoso, and R. A. Osornio-Rios, "A Hilbert transform-based smart sensor for detection, classification, and quantification of power quality disturbances," *Sensors*, vol. 13, no. 5, pp. 5507–5527, 2013.
[41] X. Jiang and H. Adeli, "Pseudospectra, MUSIC, and dynamic wavelet neural network for damage detection of highrise buildings," *Int. J. Numer. Methods Eng.*, vol. 71, no. 5, pp. 606–629, 2007.
[42] National Physical Laboratory. (2006). *Power Quality Waveform Library, 'Flicker Waveforms'*. [Online]. Available: http://resource.npl.co.uk/waveform/datafiles/flicker_waveform_library.pdf
[43] Solarmax. (Jul. 2017). *SolarMax 50C/80C/100C/300C Datasheet*. [Online]. Available: http://www.tritec-energy.com/images/content/10202002_SolarMax_C-Central_big_web_enu.pdf
[44] Ingeteam. (Jul. 2017). *Ingecon Sun Power 100 Datasheet*. [Online]. Available: http://www.ingeteam.com/Portals/0/Catalogo/Producto/Documento/PRD_1690_Archivo_ingecon-sun-power.pdf
[45] LEM. (Jul. 2017). *Current Transducer HOP 500-SB/SP1 Datasheet*. [Online]. Available: http://www.lem.com/docs/products/hop_500-sb_sp1.pdf
[46] YHDC. (Jul. 2017). *Current transformer SCT-013-010 Datasheet*. [Online]. Available: http://www.yhdc.us/ENpdf/SCT013-010-0-10A-0-1V_en.pdf

DAVID A. ELVIRA-ORTIZ (S'16) received the B.E. degree from the University of Guanajuato, Mexico, in 2013, and the M.Sc. degree (Hons.) from the Autonomus University of Queretaro, Mexico, in 2015,where he is currently pursuing the Ph.D. degree. He is also with the HSPdigital Research Group. His current research interests include hardware signal processing on FPGA, renewable energies, and power quality monitoring.

DANIEL MORINIGO-SOTELO (M'04) received the B.S. and Ph.D. degrees in electrical engineering from the University of Valladolid (UVA), Spain, in 1999 and 2006, respectively. He was a Research Collaborator on electromagnetic processing of materials with the Light Alloys Division, CIDAUT Foundation, from 2000 to 2015. He is currently with the Research Group on Analysis and Diagnostics of Electrical Grids and Installations, UVA, and the HSPdigital Research Group, Mexico. His current research interests include the fault detection and diagnostics of induction machines, power quality, and smart grids.

OSCAR DUQUE-PEREZ received the B.S. and Ph.D. degrees in electrical engineering from the University of Valladolid (UVA), Spain, in 1992 and 2000, respectively. In 1994, he joined the E.T.S. de Ingenieros Industriales, UVA, where he is currently a Full Professor with the Department of Electrical Engineering. He is also with the Research Group on Analysis and Diagnosis of Electrical Installations and Networks. His main research interests include power systems reliability, condition monitoring, and power quality.

ARTURO Y. JAEN-CUELLAR received the B.E. degree in automation, the M.S. degree in instrumentation and automatic control, and the Ph.D. degree in mechatronics from the Autonomus University of Queretaro, Queretaro, Mexico. He is currently a National Researcher with CONACYT and a full-time Professor with the Autonomus University of Queretaro. His research interests include hardware signal processing using field-programmable gate arrays, digital systems, process control, instrumentation, and the application of heuristic techniques to solve mechatronics problems.

ROQUE A. OSORNIO-RIOS (M'10) received the Ph.D. degree in mechatronics from the Autonomous University of Queretaro, Queretaro, Mexico, in 2007. He is currently a Head Professor with the Autonomus University of Queretaro. He is an advisor for over 80 theses, and has co-authored of over 90 technical papers published in international journals and conferences. His fields of interest include hardware signal processing and mechatronics. He is a fellow of the Mexican Academy of Engineering. He is also a National Researcher level 2 with the Mexican Council of Science and Technology, CONACYT. He is a part of the editorial board of Journal and Scientific and Industrial Research.

RENE DE J. ROMERO-TRONCOSO (M'07–SM'12) received the Ph.D. degree in mechatronics from the Autonomous University of Queretaro, Mexico, in 2004. He is currently a Full Professor with the Autonomous University of Queretaro, and he has been an Invited Researcher with the University of Valladolid, Spain. He is an author of two books on digital systems (in Spanish), and has co-authored of over 170 technical papers published in international journals and conferences. His fields of interest include hardware signal processing with FPGA and monitoring and diagnosis on dynamic systems. He is also a National Researcher level 3 with the Mexican Council of Science and Technology, CONACYT, and a fellow of the Mexican Academy of Engineering. He was a recipient of the 2004 Asociación Mexicana de Directivos de la Investigación Aplicada y el Desarrollo Tecnológico Nacional Award on Innovation for his work in applied mechatronics, and the 2005 IEEE ReConFig Award for his work in digital systems.